

# Mechanisms of the Antitumor Activity of Human V $\gamma$ 9V $\delta$ 2 T Cells in Combination With Zoledronic Acid in a Preclinical Model of Neuroblastoma

Emma Di Carlo<sup>1,2</sup>, Paola Bocca<sup>3</sup>, Laura Emionite<sup>4</sup>, Michele Cilli<sup>4</sup>, Giuseppe Cipollone<sup>5</sup>, Fabio Morandi<sup>3</sup>, Lizzia Raffaghello<sup>3</sup>, Vito Pistoia<sup>3</sup> and Ignazia Prigione<sup>3</sup>

<sup>1</sup>Anatomic Pathology and Molecular Medicine, Department of Medicine and Sciences of Aging, "G. d'Annunzio" University, Chieti, Italy;

<sup>2</sup>Ce.S.I. Aging Research Center, "G. d'Annunzio" University Foundation, Chieti, Italy; <sup>3</sup>Laboratory of Oncology, "Istituto Giannina Gaslini", Genoa, Italy; <sup>4</sup>Animal Model Facility, IRCCS Azienda Ospedaliera Universitaria San Martino, IST, Istituto Nazionale per la Ricerca sul Cancro, Genoa, Italy;

<sup>5</sup>Department of Biomedical Science, "G. d'Annunzio" University, Chieti, Italy

Low expression of surface major histocompatibility complex (MHC) class I molecules and defects in antigen processing machinery make human neuroblastoma (NB) cells appropriate targets for MHC-unrestricted immunotherapeutic approaches. Human T-cell receptor (TCR) V $\gamma$ 9V $\delta$ 2 lymphocytes exert MHC-unrestricted antitumor activity and are activated by phosphoantigens, whose expression in cancer cells is increased by aminobisphosphonates. With this background, we have investigated the *in vivo* anti-NB activity of human V $\gamma$ 9V $\delta$ 2 lymphocytes and zoledronic acid (ZOL). SH-SY-5Y human NB cells were injected in the adrenal gland of immunodeficient mice. After 3 days, mice received ZOL or human V $\gamma$ 9V $\delta$ 2 T cells or both agents by intravenous administration once a week for 4 weeks. A significantly improved overall survival was observed in mice receiving V $\gamma$ 9V $\delta$ 2 T cells in combination with ZOL. Inhibition of tumor cell proliferation, angiogenesis and lymphangiogenesis, and increased tumor cell apoptosis were detected. V $\gamma$ 9V $\delta$ 2 T lymphocytes were attracted to NB-tumor masses of mice receiving ZOL where they actively modified tumor microenvironment by producing interferon- $\gamma$  (IFN- $\gamma$ ), that in turn induced CXCL10 expression in NB cells. This study shows that human V $\gamma$ 9V $\delta$ 2 T cells and ZOL in combination inhibit NB growth *in vivo* and may provide the rationale for a phase I clinical trial in patients with high-risk NB.

Received 31 October 2012; accepted 7 February 2013; advance online publication 12 March 2013. doi:10.1038/mt.2013.38

## INTRODUCTION

Neuroblastoma (NB) is the most frequent extracranial solid tumor in children, with more than 50% of patients displaying metastatic disease at diagnosis.<sup>1</sup> Bone marrow is the most common site of NB metastasis.<sup>2</sup> Despite aggressive therapies, the outcome of children with metastatic NB at diagnosis still remains poor, with approximately one third of them surviving at 5 years.<sup>3</sup> Many efforts are

ongoing to develop new therapeutic strategies, and immunotherapy has attracted interest especially as adjuvant to standard frontline therapies.<sup>4</sup> A better understanding of interactions between tumor cells, tumor microenvironment and the immune system is instrumental for the development of novel therapeutic approaches aiming at potentiating anti-NB immune response while dampening tumor-driven immunosuppressive mechanisms. Indeed, different preclinical and clinical strategies of antibody-mediated and cell-mediated NB immunotherapy have been developed in the last years.<sup>4</sup>

To design appropriate immunotherapeutic protocols for human NB, the multiple mechanisms of immune evasion adopted by tumor cells must be taken into account.<sup>5–9</sup> Low expression of surface major histocompatibility complex (MHC) class I molecules and defects in the antigen processing machinery of human NB cells allow the latter cells to escape the attack of tumor-specific T cells.<sup>5,10</sup> On the other hand, downregulation of MHC class I molecules makes NB cells appropriate targets for MHC-unrestricted immunotherapeutic approaches making use of natural killer cells or T-cell receptor (TCR) gamma delta ( $\gamma\delta$ ) T cells.<sup>11–13</sup> Interferon- $\gamma$  (IFN- $\gamma$ ) can upregulate MHC class I and some components of the antigen processing machinery in cancer cells including NB cells, exert antiangiogenic activity by inducing CXCL9 and CXCL10 expression, and re-program antitumor immune responses, thus modifying the tumor microenvironment.<sup>14</sup>

In the blood of healthy subjects,  $\gamma\delta$  T cells represent 1–5% of circulating T lymphocytes and display predominantly the V $\gamma$ 9V $\delta$ 2 TCR.<sup>15</sup> V $\gamma$ 9V $\delta$ 2 T cells possess the unique capacity to recognize in a MHC-unrestricted way and be activated by natural nonpeptide phosphorylated intermediates of isoprenoid metabolism. These include exogenous prenyl pyrophosphates from bacteria and parasitic protozoa as well as endogenous prenyl pyrophosphates, e.g., isopentenyl pyrophosphate (IPP), deriving from the mevalonate pathway that operates in human cells.<sup>16</sup>

Tumor cells that produce elevated concentrations of IPP can be recognized and killed by V $\gamma$ 9V $\delta$ 2 T cells.<sup>16,17</sup> Tumor cell production of IPP can be boosted by exposure to aminobisphosphonates,

The first two authors contributed equally and the last two authors contributed equally.

Correspondence: Ignazia Prigione, Laboratory of Oncology, Istituto Giannina Gaslini, Via G. Gaslini 5, 16148 Genoa, Italy.

E-mail: [ignaziaprigione@ospedale-gaslini.ge.it](mailto:ignaziaprigione@ospedale-gaslini.ge.it)

a class of drugs that inhibit osteoclastic reabsorption.<sup>18,19</sup> The latter drugs specifically inhibit the IPP-processing enzyme pharnesyldiphosphate synthase in the mevalonate pathway leading to accumulation of IPP.<sup>20</sup> Zoledronic acid (ZOL) is an aminobisphosphonate that, besides its antiosteoclastic activity, exerts direct and indirect antitumor effects *via* inhibition of tumor growth and angiogenesis and induction of malignant cell apoptosis.<sup>21–25</sup> ZOL, especially when combined with IL-2, has a strong capacity to activate and expand human V $\gamma$ 9V $\delta$ 2 T cells displaying an effector-memory immunophenotype.<sup>26–28</sup>

V $\gamma$ 9V $\delta$ 2 T cells exert their antineoplastic activity by MHC unrestricted killing of tumor cells and antibody-dependent cellular cytotoxicity, as well as by activation of other immune effector mechanisms through cytokine release.<sup>29–31</sup> The potent antitumor activity of V $\gamma$ 9V $\delta$ 2 T cells against solid tumors,<sup>32</sup> multiple myeloma and lymphomas<sup>33</sup> supports their use in clinical trials, especially in combination with conventional chemotherapy.<sup>18,34</sup> ZOL has been clinically approved for the treatment of patients with bone metastasis from solid tumors and multiple myeloma.<sup>24,35,36</sup> So far, the combination of adoptively transferred V $\gamma$ 9V $\delta$ 2 T cells and ZOL has been tested in a few preclinical models of adult human malignancies and in a recent phase I clinical trial.<sup>28,34,37</sup>

In this study, the antitumor activity of human V $\gamma$ 9V $\delta$ 2 T cells and ZOL in combination has been investigated in an orthotopic mouse model of human NB<sup>38,39</sup> and the mechanisms involved have been identified.

## RESULTS

### Lysis of NB cell lines by ZOL-expanded V $\gamma$ 9V $\delta$ 2 T cells from normal donors and patients with NB

These experiments were carried out in preparation for the *in vivo* studies reported in the following sections. TCR V $\gamma$ 9V $\delta$ 2 cell populations were expanded *in vitro* by ZOL stimulation of peripheral blood mononuclear cells from four normal donors and three untreated patients with stage 4 NB at diagnosis. **Figure 1** shows the immunophenotype of V $\gamma$ 9V $\delta$ 2 T cell-expansions derived from three normal donors (**Figure 1a**) and from three patients with NB (**Figure 1b**), respectively. A common CD3<sup>+</sup> CD4<sup>-</sup> CD45R0<sup>+</sup> CXCR3<sup>+</sup> phenotype characterized both normal donor- and patient-derived V $\gamma$ 9V $\delta$ 2 T cells (**Figure 1a,b**, upper histogram plots). Differently, variable patterns of expression of CD8, CD27, and CD16 markers were detected in each V $\gamma$ 9V $\delta$ 2 T cell-expansion, either from normal donors (**Figure 1a**) or patients (**Figure 1b**).

Overnight pretreatment of SH-SY-5Y NB cells, subsequently used for *in vivo* experiments, and HTLA-230 NB cells with 10  $\mu$ mol/l and 50  $\mu$ mol/l ZOL, respectively, significantly increased their susceptibility to killing by V $\gamma$ 9V $\delta$ 2 T cells expanded from normal donors, at all effector: target ratios tested ( $P < 0.001$ , **Figure 1c,d**). Similar results were observed when patient derived V $\gamma$ 9V $\delta$ 2 T cells were used as effectors against ZOL sensitized SH-SY-5Y target cell line ( $P < 0.001$ , **Figure 1e**).

Patient (**Figure 1f**) and normal donor (data not shown) derived V $\gamma$ 9V $\delta$ 2 T cells lysed ZOL sensitized SH-SY-5Y NB cells *via* TCR-dependent and perforin-mediated mechanisms, as demonstrated by treatment of effector cells with anti-V $\gamma$ 9 blocking mAb or the vacuolar-type H<sup>+</sup>-ATPase inhibitor concanamycin A,

respectively. Blocking of NKG2D on V $\gamma$ 9V $\delta$ 2 T cells was ineffective (**Figure 1f**).

Finally, incubation of target cells with mevastatin, which prevents ZOL-induced IPP accumulation, during ZOL pretreatment dampened V $\gamma$ 9V $\delta$ 2 T cell-mediated lysis (**Figure 1f**).

### *In vivo* efficacy of combined administration of V $\gamma$ 9V $\delta$ 2 T cells and ZOL

To investigate *in vivo* the anti-NB activity of V $\gamma$ 9V $\delta$ 2 T cells in combination with ZOL we used an orthotopic mouse model that mimics closely the growth pattern of human NB.<sup>38,39</sup> The SH-SY-5Y NB cell line was implanted in the adrenal gland of nude/nude athymic mice because this cell line was previously well characterized for its patterns of growth and spreading following orthotopic xenograft.<sup>39</sup> Three days after tumor implantation, mice were weekly *i.v.* treated with  $5 \times 10^6$  V $\gamma$ 9V $\delta$ 2 T cells, ZOL (150  $\mu$ g/Kg), or both, in combination, for 4 weeks.

A statistically significant improvement of survival was observed in mice receiving V $\gamma$ 9V $\delta$ 2 T cells after ZOL pretreatment, in comparison with untreated mice ( $P = 0.024$ ; median survival times: 42 and 48 days for untreated and treated mice, respectively) (**Figure 2a**). In contrast, survival of mice treated with V $\gamma$ 9V $\delta$ 2 T cells (**Figure 2b**) or ZOL (**Figure 2c**) as single agents was not significantly different from that of the control group ( $P > 0.05$ ; median survival times: 43 days for V $\gamma$ 9V $\delta$ 2 T cells or ZOL treatment groups, 42 days for control group).

### Morphological and immunohistochemical analyses disclose the mechanisms underlying the *in vivo* anti-NB activity of V $\gamma$ 9V $\delta$ 2 T cells and ZOL

Tumors from nu/nu mice ( $n = 6$ ) orthotopically implanted with human NB SH-SY-5Y cells, were composed of large primitive-appearing cells growing in solid sheets and sometimes arranged in Homer-Wright pseudorosettes. Such cells displayed large vesicular nuclei and prominent nucleolus, scant cytoplasm and poorly defined cell borders (**Figure 3a**). These tumors showed high proliferative activity, as assessed by Ki-67 immunostaining (**Figure 3b** and **Table 1**), frequent cyclin D1 expression (**Figure 3c**) and a few apoptotic figures, as assessed by the TUNEL assay (**Figure 3d** and **Table 1**). Tumor growth was supported by a richly branched vascular network composed of microvessels of both murine and human origin as revealed, respectively, by anti-mouse-CD31 and anti-human-vWF immunostainings (**Figure 4a,b** and **Table 1**).

ZOL treatment ( $n = 6$ ) resulted in frequent ischemic-hemorrhagic foci of the tumor masses (**Figure 3e**), associated with significant ( $P < 0.05$ ) impoverishment of human vWF<sup>+</sup> endothelial microvessels (**Figure 4e** and **Table 1**). In contrast, counts of CD31<sup>+</sup> murine microvessels did not differ significantly in ZOL treated mice compared with controls (**Figure 4d** and **Table 1**). ZOL treatment virtually abolished tumor cell expression of VEGF-A compared with controls (**Figure 4f** and **Table 1**), whereas tumor cell proliferation and Cyclin D1 expression appeared substantially unchanged (**Figure 3f,g**; **Table 1**) along with the frequency of apoptotic events (**Figure 3h** and **Table 1**) which may also involve endothelial cells (inset in **Figure 3h**).

Injection of human V $\gamma$ 9V $\delta$ 2 T lymphocytes ( $n = 7$ ) promoted very small collapses of the tumor tissues (**Figure 3i**) in association

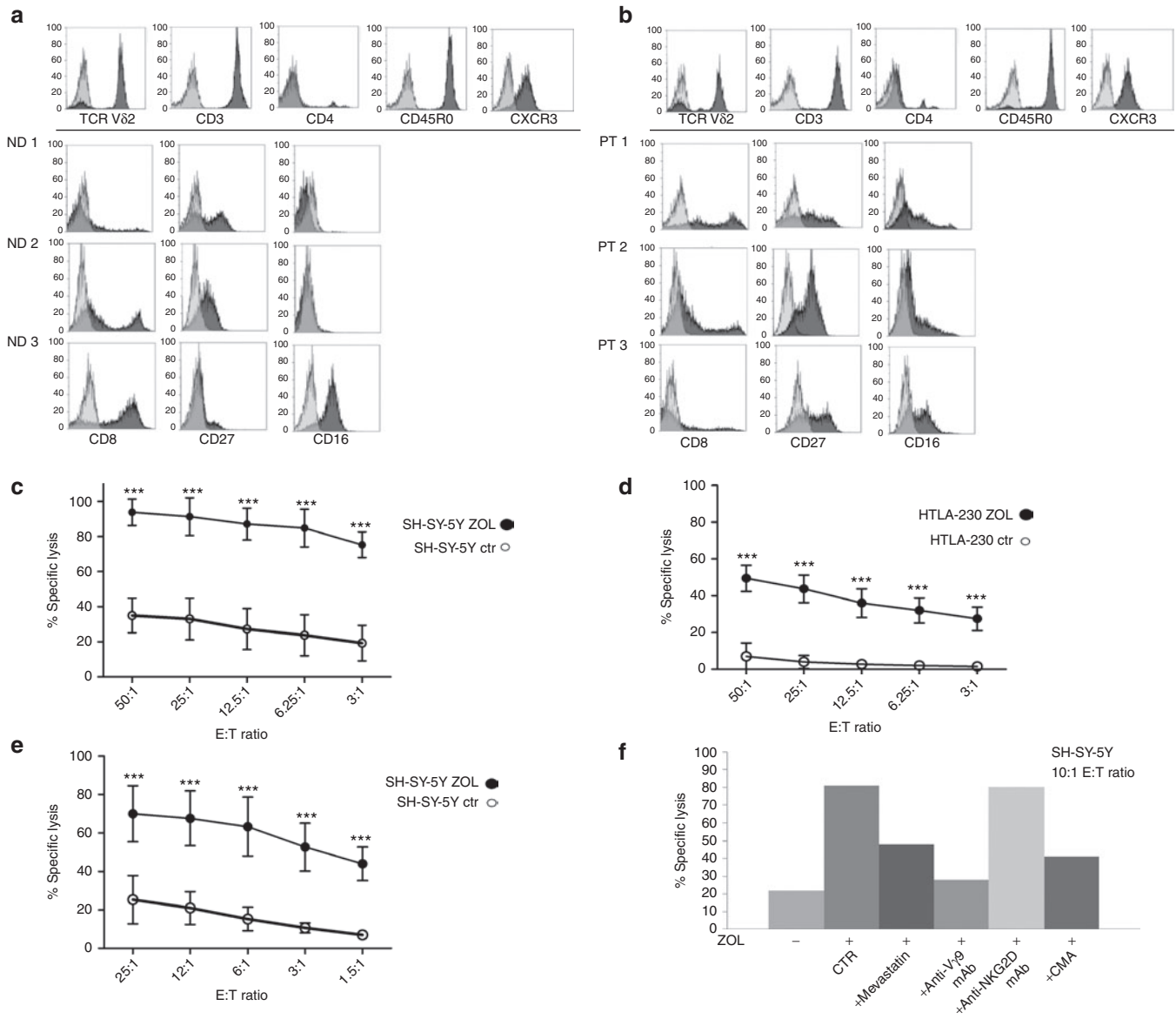


**Figure 1** Immunophenotypic and cytotoxic properties of  $V\gamma 9V\delta 2$  T cells expanded *in vitro* by ZOL stimulation of PBMC from normal donors and patients with NB. PBMC from normal donors and patients with NB at diagnosis were cultured in the presence of ZOL and IL-2. Proliferating cells were expanded in IL-2 containing medium. Immunophenotype and cytotoxicity were tested after 10/12 day culture. **(a,b)**: immunophenotypic profiles of  $V\gamma 9V\delta 2$  T cells expanded from **(a)** three normal donors (ND) and **(b)** three patients with NB (Pt). Upper histogram plots in **(a)** and **(b)** show markers, from a representative sample, expressed with the same pattern in each  $V\gamma 9V\delta 2$  T cell expansion. The other histogram plots show markers differently expressed in each  $V\gamma 9V\delta 2$  T cell expansion. Grey histograms represent isotype controls and black histograms are the specific stainings. **(c,d)**  $V\gamma 9V\delta 2$  T cells expanded from four normal donors were tested for cytotoxic activity against untreated and ZOL-sensitized SH-SY-5Y and HTLA-230 human NB cells. Results are expressed as mean percentage of specific lysis  $\pm$  SD from four independent experiments ( $***P < 0.001$ ). **(e)**  $V\gamma 9V\delta 2$  T cells expanded from three patients with NB were tested for cytotoxic activity against untreated and ZOL-sensitized SH-SY-5Y NB cells. Results are expressed as mean percentage of specific lysis  $\pm$  SD from three independent experiments ( $***P < 0.001$ ). **(f)** Cytotoxic activity of  $V\gamma 9V\delta 2$  T cells expanded from one patient with NB against ZOL-sensitized SH-SY-5Y NB cells was tested, at 10:1 E:T ratio, after preincubation of effectors with medium (CTR) or with anti-TCR  $V\gamma 9$  mAb, or anti-NKG2D mAb or concanamycin A (CMA) and after preincubation of target cells with Mevastatin. Results from one representative experiment of three performed are shown. NB, neuroblastoma; PBMC, peripheral blood mononuclear cells.

with a significantly ( $P < 0.05$ ) increased tumor cell apoptosis versus controls only (Figure 3l and Table 1). Tumor cell proliferation and cyclin D1 expression (Figure 3j,k), along with VEGF-A expression (Figure 4i), were basically unchanged in comparison with control, and the micro-vascular network integrity was substantially unaltered in both murine and human components (Figure 4g,h and Table 1).

Tumors from mice treated with ZOL 16 hours before human  $V\gamma 9V\delta 2$  T lymphocyte infusion were harvested 6 hours after the administration of the latter cells ( $n = 9$ ). This combined treatment induced a peculiar “worm-eaten” feature of the tumor tissue (Figure 3m) in association with significant inhibition of tumor cell proliferation ( $P < 0.05$ ) and reduced cyclin D1 expression (Figure 3n,o and Table 1) compared with tumors

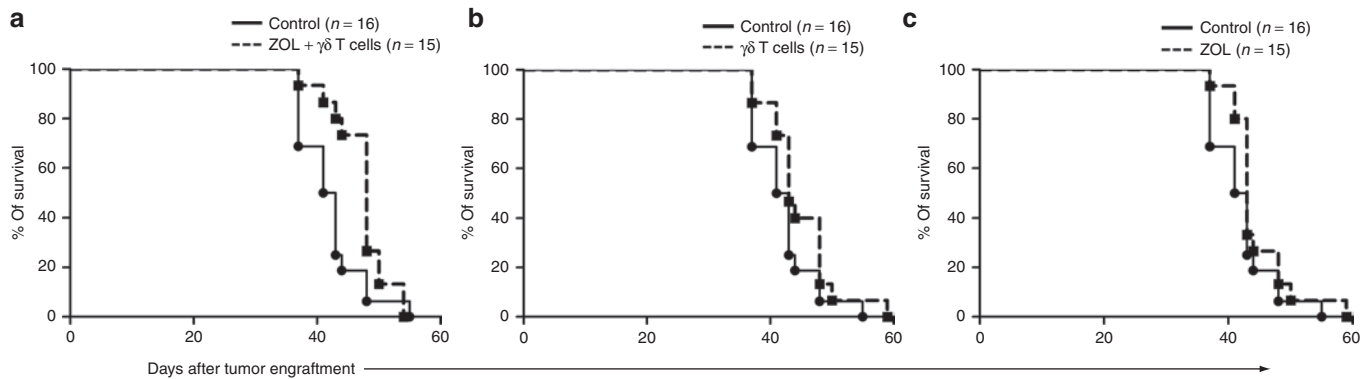


**Figure 2** Survival of mice orthotopically engrafted with SH-SY-5Y cells treated with ZOL and human  $V\gamma 9V\delta 2$  T cells as single agents or in combination. Five-week-old female athymic (nude/nude) Balb/c mice were orthotopically xenografted in the left adrenal gland with human SH-SY-5Y NB cells. Three days after, mice were randomized into four groups receiving different treatments (one weekly treatment for 4 weeks). Pooled results from two different experiments are shown. The overall survival of mice receiving human  $V\gamma 9V\delta 2$  T cells and ZOL in combination was significantly higher than that of control mice ( $P = 0.024$ , Kaplan–Meier, log-rank test) (**a**). In contrast, the overall survival of mice treated with  $V\gamma 9V\delta 2$  T cells alone (**b**) or ZOL alone (**c**) did not differ significantly from that of control mice.

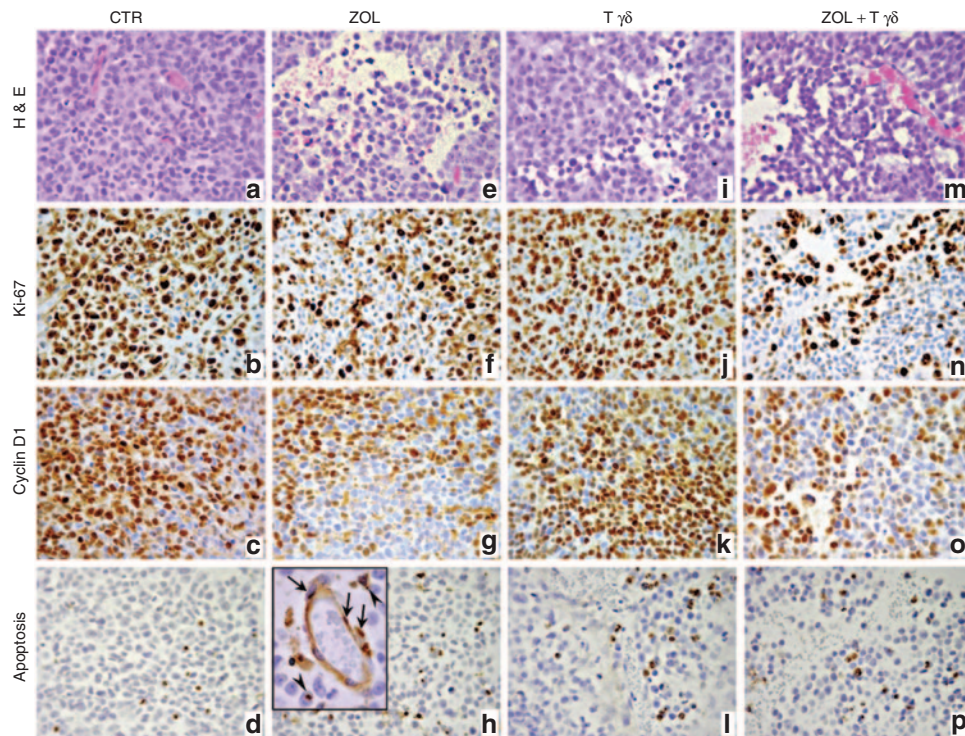


**Figure 3** Histologic features and immunohistochemical analysis of proliferative activity and apoptosis of tumors developed in mice that received treatments with ZOL and/or human  $V\gamma 9V\delta 2$  T cells. H&E staining of tumors developed after orthotopic injection of SH-SY-5Y NB cells in untreated mice (**a**) and in mice treated with ZOL (**e**),  $V\gamma 9V\delta 2$  T cells (**i**) or ZOL +  $V\gamma 9V\delta 2$  T cells (**m**). Immunostaining with anti-Ki-67 and anti-Cyclin D1 Abs of tumors developed in untreated mice (**b,c**) and in mice treated with ZOL (**f,g**),  $V\gamma 9V\delta 2$  T cells (**j,k**) or ZOL +  $V\gamma 9V\delta 2$  T cells (**n,o**). TUNEL assay performed on tumors developed in untreated mice (**d**) and in mice treated with ZOL (**h**; inset panel: arrows, endothelial cells; arrowheads, neoplastic cells),  $V\gamma 9V\delta 2$  T cells (**l**) or ZOL +  $V\gamma 9V\delta 2$  T cells (**p**). (**a–p**:  $\times 400$ ; inset panel in **h**:  $\times 1,000$ ). Abs, antibodies; H&E, hematoxylin and eosin.

from untreated or single agent treated mice. Tumor cell apoptosis was significantly ( $P < 0.05$ ) increased in mice treated with ZOL and human  $V\gamma 9V\delta 2$  T lymphocytes (**Figure 3p** and **Table 1**) compared with tumors from untreated, but not single agent treated, mice. Tumor masses from mice that received the combined treatment showed scarce to absent VEGF-A expression (**Figure 4l**) and a severely compromised micro-vascular network, because (i) murine microvessels were significantly ( $P <$

0.05) reduced in comparison with untreated or single agent treated animals, and (ii) human microvessels were significantly ( $P < 0.05$ ) reduced when compared with tumors from untreated or human  $V\gamma 9V\delta 2$  T lymphocyte treated mice (**Figure 4j,k** and **Table 1**).

Immunohistochemistry for D2-40/podoplanin revealed that control tumors were endowed with a robust lymphatic microvasculature of human origin and also showed a distinct expression

**Table 1** Immunohistochemical analyses of tumors developed after SH-SY-5Y cell injection in the adrenal gland of athymic nu/nu mice untreated or treated with ZOL, human Vγ9Vδ2 T cells or both

	ctr	ZOL	Tγδ	ZOL + Tγδ	ANOVA <sup>a</sup> (P value)
Murine blood vessels <sup>b</sup>	7.9 ± 3.1	3.7 ± 2.0	7.0 ± 2.6	1.0 ± 0.4 <sup>c,d,e</sup>	<0.001
Human blood vessels <sup>b</sup>	12.0 ± 3.6	5.0 ± 2.5 <sup>c</sup>	10.2 ± 4.2	1.5 ± 1.0 <sup>c,e</sup>	<0.001
Human lymphocytes vessels	14.5 ± 4.0	6.8 ± 3.0 <sup>c</sup>	12.0 ± 3.5	2.0 ± 1.3 <sup>c,d,e</sup>	<0.001
γδ T lymphocytes	NA <sup>f</sup>	NA	6.0 ± 2.5	14.5 ± 4.0 <sup>c</sup>	
Human cytokines <sup>g</sup>					
IFN-γ	–	–	±	++	
MIG/CXCL9	–	–	–	–	
IP-10/CXCL10	–	–	–	++	
Human angiogenic factors					
VEGF-A	++	±	++	±	
VEGF-C	++	±	++	±	
Proliferation index <sup>b</sup>	85.4 ± 8.6%	71.4 ± 7.2%	80.0 ± 8.3%	54.3 ± 7.5% <sup>c,d,e</sup>	<0.001
Apoptotic index <sup>b</sup>	7.2 ± 2.5%	9.8 ± 3.0%	13.2 ± 3.3% <sup>c</sup>	12.6 ± 2.4% <sup>c</sup>	<0.001

<sup>a</sup>P < 0.001 One-way analysis of variance (ANOVA) for comparisons between four groups. <sup>b</sup>Assessment of cytokine and angiogenic factor expression and counts of microvessels and γδ T cells were performed at ×400 in a 0.180 mm<sup>2</sup> field. At least three samples (one sample/tumor growth area) and 8–10 randomly chosen fields/sample were evaluated. Results are expressed as mean ± SD of CD31 (murine blood vessels), or vWF (human blood vessels), or D2-40/podoplanin (human lymphatic vessels) positive microvessels per field; or TCRγδ positive cells per field; or Ki-67 or TUNEL positive cells/number of total cells evaluated on formalin-fixed sections by immunohistochemistry. <sup>c</sup>P < 0.05 Tukey test compared with tumors from untreated (ctr) mice. <sup>d</sup>P < 0.05 Tukey test compared with tumors from ZOL only treated mice. <sup>e</sup>P < 0.05 Tukey test compared with tumors from Tγδ lymphocyte only treated mice. <sup>f</sup>Not applicable. <sup>g</sup>The expression of cytokines and angiogenic factors was defined as absent (–), scarce (±), moderate (+), or frequent (++) on paraffin embedded (VEGF-A and VEGF-C) or cryostat (IFN-γ, MIG/CXCL9, IP-10/CXCL10) sections stained with the corresponding antibody.

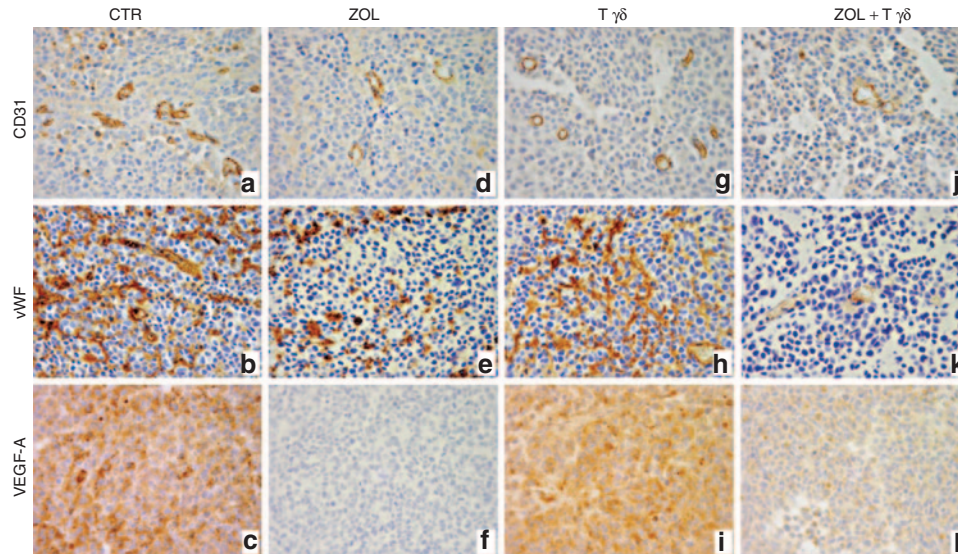


**Figure 4** Vascular network in tumors developed in mice that after orthotopic engraftment of SH-SY-5Y cells received treatments with ZOL and/or human Vγ9Vδ2 T cells. Immunostaining with anti-CD31, anti-vWF and anti-VEGF-A Abs of tumors developed after orthotopic injection of SH-SY-5Y NB cells in untreated mice (**a**, **b** and **c**, respectively) and in mice treated with ZOL (**d–f**), Vγ9Vδ2 T cells (**g–i**) or ZOL + Vγ9Vδ2 T cells (**j–l**). (**a–l**: ×400). Abs, antibodies.

of VEGF-C (**Figure 5a,b** and **Table 1**). Similar features were observed in tumors from Vγ9Vδ2 T lymphocyte only treated mice (**Figure 5e,f**), whereas tumors from ZOL treated mice showed significant reduction of lymphatic vasculature ( $P < 0.05$ ) and reduced VEGF-C expression (**Figure 5c,d** and **Table 1**) when compared with control tumors. Finally, in tumors from mice receiving the combined treatment VEGF-C expression was reduced similarly to that observed in tumors from animal receiving ZOL only, whereas

lymphatic vasculature was significantly decreased ( $P < 0.05$ ) compared with untreated or single agent treated animals (**Figure 5h,g** and **Table 1**).

In summary, the most remarkable and significant anti-NB effects were obtained when ZOL and Vγ9Vδ2 T cells were administered in combination. ZOL alone showed significant antiangiogenic activity, whereas Vγ9Vδ2 T cells administered alone affected significantly tumor cell apoptosis.

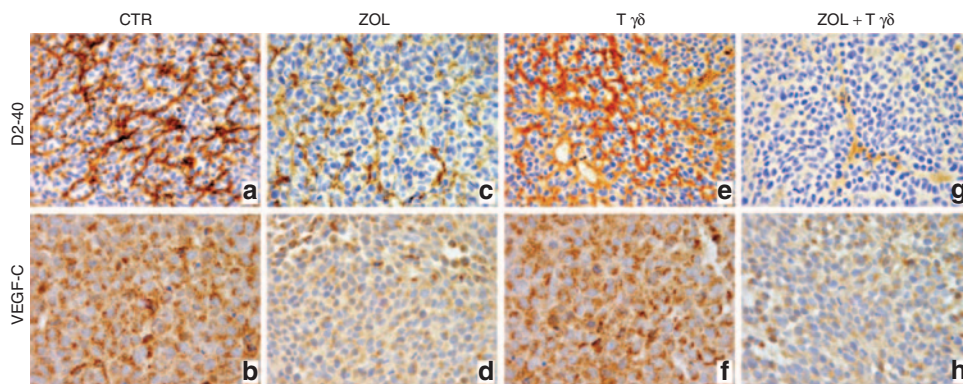


**Figure 5** Lymphatic vessel network and VEGF-C expression in tumors developed in mice that after orthotopic engraftment of SH-SY-5Y cells received treatments with ZOL and/or human  $V\gamma9V\delta2$  T cells. Immunostaining with anti-D2-40 and anti-VEGF-C Abs of tumors developed (**a,b**) in untreated mice and (**c,d**) in mice treated with ZOL, (**e,f**)  $V\gamma9V\delta2$  T cells or (**g,h**) ZOL +  $V\gamma9V\delta2$  T cells. (**a,c,e,g**:  $\times 400$ ; **b,d,f,h**:  $\times 630$ ). Photographs are representative of the staining detected in at least 6 out of 8 randomly chosen fields/tumor sample. Three samples were examined for each experimental group. Abs, antibodies.

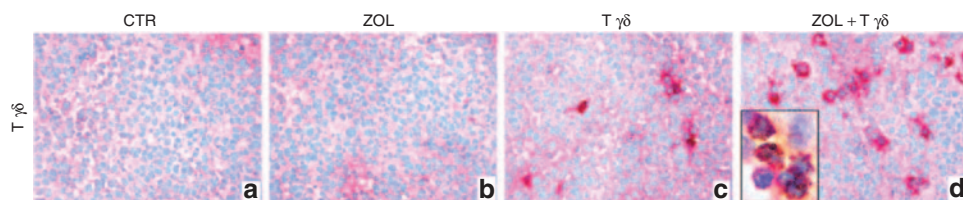


**Figure 6** Detection and characterization of human  $T\gamma\delta$  lymphocytes in the tumor masses developed in mice that after orthotopic engraftment of SH-SY-5Y cells received human  $V\gamma9V\delta2$  T cells and/or ZOL. Immunostaining with anti- $TCR\gamma\delta$  Ab of tumors developed in (**a**) untreated mice and (**b**) in mice treated with (**c**) ZOL,  $V\gamma9V\delta2$  T cells or ZOL +  $V\gamma9V\delta2$  T cells (**d**). Double immunostaining with anti- $TCR\gamma\delta$  (red) and anti-TIA-1 (intracytoplasmic granular brown dots) Abs (inset in **d**). (**a-d**:  $\times 400$ ; inset in **d**:  $\times 1,000$ ). Abs, antibodies.

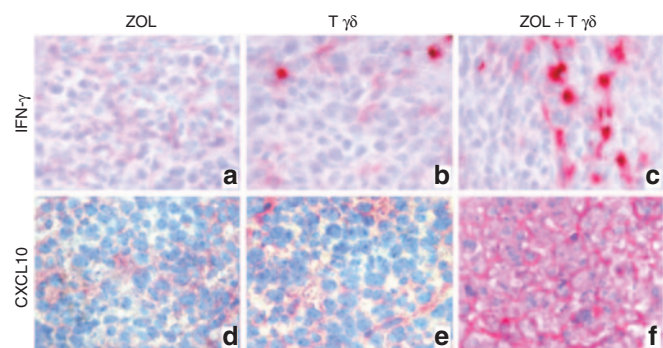


**Figure 7** Detection of IFN- $\gamma$  and CXCL10 in the tumor masses developed in mice that, after orthotopic engraftment of SH-SY-5Y cells, received ZOL, human  $V\gamma9V\delta2$  T cells or both. Immunostaining with anti-IFN- $\gamma$  and anti-CXCL10 Abs in tumors from mice treated with (**a,d**) ZOL or (**b,e**)  $V\gamma9V\delta2$  T cells only and in tumors from mice treated with (**c,f**) ZOL +  $V\gamma9V\delta2$  T cells. (**a-f**:  $\times 1,000$ ). Abs, antibodies.

### Perturbation of tumor microenvironment by infiltrating $V\gamma9V\delta2$ T lymphocytes in mice treated with $V\gamma9V\delta2$ T cells and ZOL

Tumor localization of adoptively transferred human  $V\gamma9V\delta2$  T lymphocytes, alone or combined with ZOL, and their influence on tumor microenvironment were investigated by immunohistochemical analyses of tumor masses from NB orthotopically implanted mice. Mice were treated with ZOL 16 hours before receiving or not human  $V\gamma9V\delta2$  T lymphocytes, and were sacrificed 6 hours after the completion of the third cycle of therapy.

By contrast with tumors developed in untreated (**Figure 6a**) or ZOL treated mice (**Figure 6b**), tumors developed in mice receiving human  $V\gamma9V\delta2$  T lymphocytes alone (**Figure 6c**), or in combination with ZOL (**Figure 6d**), were infiltrated by human  $\gamma\delta$  T lymphocytes. Such infiltration was significantly ( $P < 0.05$ ) higher in tumors from mice receiving the combined treatment (**Figure 6d** and **Table 1**) and most of  $\gamma\delta$  T lymphocytes expressed the cytotoxic molecule T-cell intracellular antigen-1 (TIA-1), as revealed by  $TCR\gamma\delta$ /TIA-1 double staining (inset in **Figure 6d**). In addition, immunohistochemical examination of serial tissue sections showed that hIFN- $\gamma$  production was distinct in tumor masses from mice receiving the combined treatment that appeared infiltrated by  $\gamma\delta$  T lymphocytes (**Figure 7c** and **Table 1**), whereas it was barely detectable in the tumors from mice receiving  $V\gamma9V\delta2$  T lymphocytes alone (**Figure 7b**) and obviously absent in tumors from ZOL treated (**Figure 7a**) or control animals (**Table 1**). Analyses of IFN- $\gamma$  inducible chemokine production revealed that CXCL10/IP10 was detectable in the cytoplasm of tumor cells from mice receiving the combined treatment (**Figure 7f** and **Table 1**), whereas it was absent in tumors from  $V\gamma9V\delta2$  T lymphocytes treated mice (**Figure 7e**) and in tumors from ZOL treated (**Figure 7d**) or control animals (data not shown). In contrast, expression the IFN- $\gamma$  inducible anti-angiogenic chemokine CXCL9 was not detected in tumors from any group of mice (**Table 1**).

Analyses of murine tumor infiltrating leukocytes, performed with anti-F4/80 and anti-pan-natural killer cells, revealed a scarce to moderate macrophage infiltrate at the tumor border and few macrophages penetrating the innermost areas, whereas natural

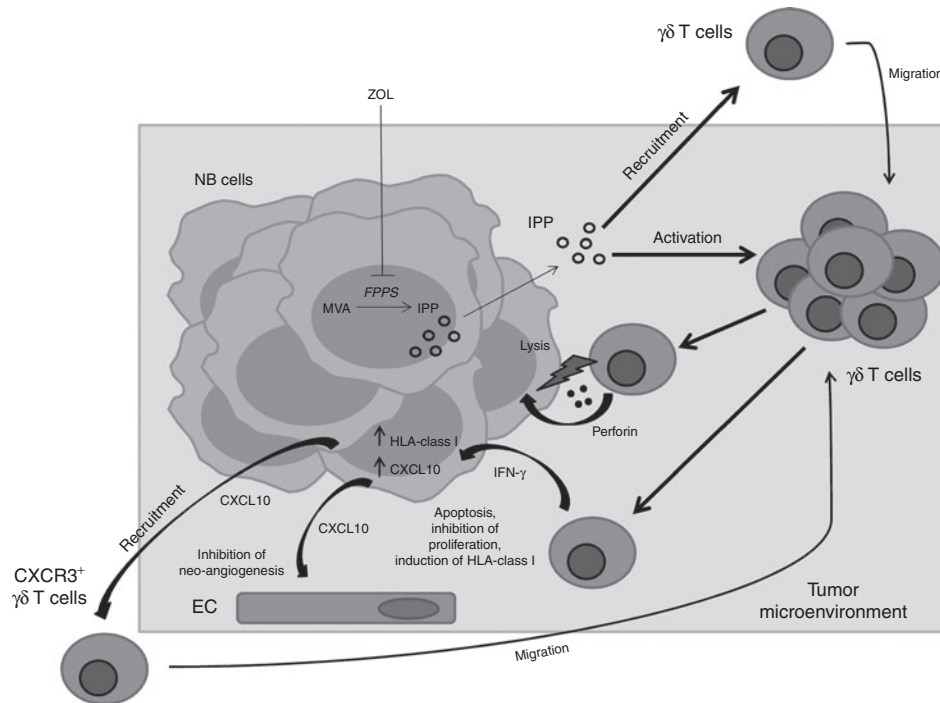


**Figure 8** A model for the effects of combined treatment with ZOL and human  $V\gamma9V\delta2$  T cells on NB tumor microenvironment. ZOL-mediated inhibition of FPPS results in intracellular accumulation of upstream metabolites of the MVA pathway including IPP, which activates and attracts  $V\gamma9V\delta2$  T cells. The latter cells kill tumor cells through a perforin-dependent mechanism and release IFN- $\gamma$  that may be involved in inhibition of NB cell proliferation and/or induction of apoptosis.  $V\gamma9V\delta2$  T cell-secreted IFN- $\gamma$  upregulates HLA class I expression on NB cells thus increasing their immunogenicity, and induces CXCL10 expression in tumor cells. CXCL10 inhibits neo-angiogenesis by binding to CXCR3 on endothelial cells and recruits a new wave of CXCR3<sup>+</sup>  $V\gamma9V\delta2$  T cells to the tumor site. EC, endothelial cells; FPPS, farnesyl pyrophosphate synthase; IPP, isopentenyl pyrophosphate; MVA, mevalonate.

killer cells were completely absent (data not shown). No relevant differences emerged in the content of murine infiltrating leukocytes within tumors from the different treatment groups (data not shown).

These data demonstrate that (i) i.v. injected human  $V\gamma9V\delta2$  T lymphocytes are able to migrate into NB-tumor masses grown in orthotopically xenografted mice; (ii) the tumor localization of i.v. injected human  $V\gamma9V\delta2$  T lymphocytes is potentiated by animal pretreatment with ZOL; and (iii) tumor localized  $V\gamma9V\delta2$  T cells can exert their functional programs and interfere with tumor microenvironment.

## DISCUSSION

Few studies have addressed the preclinical anti-NB activity of human  $\gamma\delta$  T lymphocytes or ZOL. Treatment of immunodeficient mice carrying human metastatic NB with human  $\gamma\delta$  T cells from normal individuals was ineffective.<sup>40</sup> Likewise, ZOL alone administered in a NB murine model of bone invasion inhibited osteoclast activity and tumor cell proliferation, but did not improve survival.<sup>21</sup> Finally, it has been reported that ZOL sensitizes NB-derived tumor-initiating cells to cytolysis mediated by human  $V\gamma9V\delta2$  T cells.<sup>37</sup>

We asked whether the combination of human  $V\gamma9V\delta2$  T lymphocytes and ZOL could exert synergistic anti-NB effects *in vivo* based upon the notion that ZOL may sensitize tumor cells to  $V\gamma9V\delta2$  T cell-mediated lysis. Indeed, we showed that  $V\gamma9V\delta2$  T lymphocytes with an effector/central memory phenotype could

be expanded from peripheral blood of normal individuals and patients with NB upon incubation with ZOL, and that these effector cells killed more efficiently NB cells that had been pretreated with ZOL. Recognition and lysis of NB cells by  $V\gamma9V\delta2$  T lymphocytes were found to depend on engagement of TCR but not NKG2D, release of cytotoxic granules, and ZOL-induced IPP accumulation in tumor cells. Taken together, these results are consistent with previous reports in other tumor models.<sup>16,18</sup>

*In vivo* experiments were next carried out using an orthotopic human NB model in immunodeficient mice whereby malignant cells are implanted in the adrenal gland capsule.<sup>38,39</sup> Mice received ZOL alone or  $V\gamma9V\delta2$  T cells alone or both, with ZOL administered 16 hours before  $V\gamma9V\delta2$  T lymphocytes to allow ZOL-mediated tumor cell sensitization. The survival of human NB carrying mice was significantly improved only by ZOL and  $V\gamma9V\delta2$  T cells in combination, pointing to the therapeutic synergism of these agents. However, ZOL or  $V\gamma9V\delta2$  T cells administered alone exerted significant effects on tumor angiogenesis or tumor cell apoptosis, respectively.

Tumor blood microvessels were lined by tumor-derived or host-derived endothelial cells, consistently with previous studies showing that human NB cells can transdifferentiate into endothelial cells carrying the same genetic abnormalities, e.g., *MYCN* amplification, through a phenomenon known as vascular mimicry.<sup>41,42</sup> ZOL alone significantly reduced the proportion of human blood microvessels, without any additional effect observed in mice treated with ZOL and  $V\gamma9V\delta2$  T cells. NB tumors from control

mice showed a rich network of human lymphatic microvessels that was significantly inhibited by ZOL alone and even more by ZOL and V $\gamma$ 9V $\delta$ 2 T cells in combination. Consistent with these findings, ZOL treatment reduced expression of VEGF-A and VEGF-C, that are crucial mediators of angiogenesis and lymphangiogenesis, respectively.<sup>43,44</sup>

Although inhibition of VEGF-A expression is a well-known component of the antitumor activity of ZOL,<sup>36</sup> the finding that the latter drug dampened VEGF-C expression in a mouse model of a human malignancy is novel and warrants further investigation. In this respect, inhibition of VEGF-C expression was reported in a rat model of oral wound healing as result of the impact of ZOL-mediated osteoclast suppression in the bone marrow microenvironment.<sup>45</sup>

Only ZOL and V $\gamma$ 9V $\delta$ 2 T cells in combination decreased significantly mouse derived blood microvessels in the tumor microenvironment. The finding that ZOL alone failed to inhibit formation of the latter microvessels is so far unexplained and warrants further investigation.

V $\gamma$ 9V $\delta$ 2 T cells alone increased significantly tumor cell apoptotic index and this effect was not amplified by their combination with ZOL. Tumor cell proliferation was unaffected by the single agents whereas it was significantly inhibited by ZOL and V $\gamma$ 9V $\delta$ 2 T cells.

Taken together, these results indicate that the synergistic therapeutic activity of the latter agents was attributable to *de novo* inhibition of tumor cell proliferation and mouse derived blood microvessel formation, as well as to augmented inhibition of human lymphatic microvessel network compared with ZOL alone.

Histological and immunohistochemical studies provided insight into the mechanisms underlying the synergism between ZOL and V $\gamma$ 9V $\delta$ 2 T cells. Tumors from mice treated with the latter combination were found to contain significantly higher numbers of human V $\gamma$ 9V $\delta$ 2 T cells than tumors from mice receiving V $\gamma$ 9V $\delta$ 2 T cells alone. These infiltrating lymphocytes expressed the cytotoxic granule associated molecule TIA-1 and IFN- $\gamma$ , whereas NB cells expressed at high level CXCL10, but not CXCL9.<sup>46</sup> These results support the following *scenario* (Figure 8): (i) ZOL induces accumulation in tumor cells of IPP, which activates and attracts V $\gamma$ 9V $\delta$ 2 T cells, as previously shown in a breast cancer model;<sup>19</sup> (ii) the latter cells can kill NB cells through a perforin dependent mechanism and release IFN- $\gamma$ , that in turn induces CXCL10 expression in tumor cells; (iii) IFN- $\gamma$  may be involved in inhibition of NB cell proliferation and/or induction of apoptosis;<sup>14</sup> (iv) CXCL10 can inhibit neo-angiogenesis by binding to CXCR3 on endothelial cells and recruit a new wave of CXCR3<sup>+</sup> V $\gamma$ 9V $\delta$ 2 T cells to the tumor site. An implication of this model is that V $\gamma$ 9V $\delta$ 2 T cell-derived IFN- $\gamma$  can upregulate HLA class I expression on NB cells thus increasing their immunogenicity.<sup>5</sup>

This study may provide the rationale for the design of a phase I clinical trial based upon administration of *in vitro* expanded autologous V $\gamma$ 9V $\delta$ 2 T cells together with ZOL in patients with metastatic NB and low tumor burden. Although caution is needed due to the potential interference of ZOL with actively growing bones, a phase I study combining ZOL and low-dose cyclophosphamide in patients with NB has recently been published with encouraging results.<sup>47</sup>

The therapeutic protocol used in our study may be improved as follows in the perspective of the clinical application: (i) V $\gamma$ 9V $\delta$ 2 T cells can be infused more frequently than weekly (e.g., every other day) to allow a continuous trafficking of these cells to the tumor site and administered for longer time frames<sup>34</sup> (ii) bisphosphonates including ZOL have high tropism for bone matrix leading to low plasma concentrations.<sup>48</sup> It is therefore conceivable that the therapeutic activity of ZOL can be increased by targeting the drug to the tumor site in nanoparticles coated with tumor-specific molecules, for example anti-GD2 antibody to NB cells.<sup>49</sup>

## MATERIALS AND METHODS

**Cell lines.** The human NB cell lines SH-SY-5Y<sup>39</sup> and HTLA-230 (kindly provided by Professor Emil Bogenmann) were cultured in Dulbecco's modified Eagle's medium (EuroClone, Milan, Italy) supplemented with 10% fetal bovine serum (Invitrogen, Carlsbad, CA), HEPES buffer, L-glutamine, penicillin-streptomycin, and nonessential aminoacids (EuroClone).

**In vitro V $\gamma$ 9V $\delta$ 2 T cell-expansion.** Peripheral blood mononuclear cells were isolated from blood samples of normal donors or untreated patients with stage 4 NB at diagnosis by Ficoll (Sigma-Aldrich, St Louis, MO) density centrifugation. Samples were taken after permission in accordance with informed consent and the study was approved by the local Ethical Committee. Cells were resuspended in RPMI 1640 supplemented with L-glutamine, penicillin-streptomycin, nonessential aminoacids (EuroClone) and 5% pooled human AB serum (complete medium). To expand TCR V $\gamma$ 9V $\delta$ 2 cells, peripheral blood mononuclear cells were resuspended in complete medium and cultured in the presence of ZOL (5  $\mu$ mol/l, Enzo Life Sciences; Vinci-Biochem, Italy) and 50 U/ml of recombinant (r) hIL2 (PROLEUKIN, Novartis FarmaS.p.A., Origgio, Italy) in 96-well round bottom microtiter plates (BD Falcon, BD Biosciences, NJ). Proliferating T cells were maintained in IL-2 containing medium. The immunophenotype of proliferating T cells was checked using anti-TCR V $\delta$  and CD3 monoclonal antibodies. Cultures containing higher than 90% TCR V $\delta$ 2<sup>+</sup> cells were used for further experiments, at least 2 weeks after ZOL stimulation.

**Flow cytometry.** The following monoclonal antibodies were used: CD3 PE-Cy7, CD16 FITC, (Beckman-Coulter, Marseille, France), anti-TCR V $\delta$ 2PE, CD45R0 APC, CD27 PE, CXCR3 FITC (BD Biosciences, San Jose, CA), MultiMix Triple Colour Reagent Anti Human CD3/CD4/CD8 (Dako, Glostrup, Denmark). Cells were resuspended in Dulbecco's phosphate-buffered saline (Sigma-Aldrich) with 1% fetal bovine serum (staining solution) and stained with specific monoclonal antibodies for 30 minutes in the dark at 4 °C. Cells were then washed once with staining solution and analyzed by flow cytometry. Isotype matched fluochrome-conjugated murine Ig were used as negative controls. Flow cytometric analyses were performed by FACS Calibur cytometer (BD Biosciences) and data were analyzed by CellQuest (BD Biosciences) or Kaluza (Beckman-Coulter) softwares. Results were expressed as percent of positive cells.

**Cytotoxicity assays.** Cytotoxicity assays were performed using the 4 hours <sup>51</sup>Cr-release test.<sup>50</sup> V $\gamma$ 9V $\delta$ 2 T cells *in vitro* expanded by ZOL, from normal donors and patients with NB, were used as effectors. Human NB cell lines, either untreated or treated overnight with ZOL (10–50  $\mu$ mol/l) were used as targets. Effector cells were seeded in duplicate at different concentration in 96-well V-bottom microtiter plates (BD Falcon) together with 5  $\times$  10<sup>3</sup> <sup>51</sup>Cr-labeled target cells in a final volume of 200  $\mu$ l. In some experiments, effector cells were incubated with anti-TCR V $\gamma$ 9 (clone 7A5; Pierce Endogen, Rockford, IL) or anti-NKG2D blocking monoclonal antibodies (R&D Systems, Minneapolis, MN) before being added to <sup>51</sup>Cr-labeled target cells. To inhibit perforin-mediated cytotoxicity, V $\gamma$ 9V $\delta$ 2 T cells were incubated with concanamycin A (100 ng/ml; Sigma), an inhibitor



of vacuolar-type H<sup>+</sup>-ATPase, for 2 hours at 37 °C before being added to <sup>51</sup>Cr-labeled target cells. To inhibit IPP-mediated target cell recognition by Vγ9Vδ2 T cells, Mevastatin (MEV, 25 μ; Sigma) was added to target cells 6 hours before and during ZOL pretreatment. Concanamycin A or MEV were re-added during cytotoxicity assay. Results were expressed as percentage of specific lysis.

**In vivo studies.** Five-week-old female athymic (nude/nude) Balb/c mice (Harlan Laboratories S.r.l., S. Pietro al Natisone, Italy) were anesthetized with ketamine (Imalgene 1000; Merial Italia SpA, Milan, Italy) subjected to laparotomy and orthotopically xenografted in the left adrenal gland with human SH-SY-5Y NB cells (1.2 × 10<sup>6</sup> cells/mouse suspended in 10 μl serum-free culture medium). Three days after cell inoculation, mice were randomized into four groups: (i) untreated mice, receiving normal saline, (ii) mice treated with ZOL (Zometa from Novartis, Basel, Switzerland; 150 μg/Kg), (iii) mice treated with Vγ9Vδ2 T cells (5 × 10<sup>6</sup>/mouse in 100 μl serum-free culture medium), and (iv) mice treated with Vγ9Vδ2 T cells (5 × 10<sup>6</sup>/mouse) 16 hours after Zometa (150 μg/Kg) injection. All treatments were performed by intravenous administration once a week for 4 weeks. Mice were inspected at least twice weekly for tumor development and sacrificed by cervical dislocation when signs of poor health or abdominal dilatation were observed.

This protocol was reviewed and approved by Ethical Committee of National Cancer Institute (Genova, Italy) and by Italian Ministry of Health.

**Morphological and immunohistochemical analysis.** Histological and immunohistochemical studies were performed on tumor masses explanted from mice 6 hours after the third cycle of therapy.

NB tumor masses derived from untreated and treated mice were fixed in 4% neutral buffered formalin or frozen in OCT compound. Formalin fixed tissues were, then, embedded in paraffin, sectioned at 4 μm, and stained with hematoxylin and eosin (Sigma).

For immunohistochemistry on the formalin-fixed, paraffin-embedded samples, sections were incubated for 30 minutes with mouse anti-human Ki-67, mouse anti-human von Willebrand Factor (vWF), mouse anti-human D2-40/podoplanin (Dako), rat anti-mouse CD31 (Dianova, Hamburg, Germany), rabbit anti-human cyclin D1/Bcl-1 (Thermo Scientific, Fremont, CA), rabbit anti-human VEGF-A (Santa Cruz, Santa Cruz, CA), rabbit anti-human VEGF-C (Zymed, San Francisco, CA), rat anti-mouse F4/80 (Caltag Laboratories, Burlingame, CA), and rat anti-mouse CD49b (Pan-NK cells, clone DX5; Pharmingen, San Diego, CA) antibodies.

For immunohistochemistry on the frozen samples, cryostat sections were fixed in acetone for 10 minutes. After washing in PBS/Tween-20, sections were stained with mouse anti-human TCRγδ (clone B1) (BD, Franklin Lakes, NJ), goat anti-human IFN-γ (Santa Cruz), rabbit anti-human MIG/CXCL9 (PeproTech, Rocky Hill, NJ), or mouse anti-human IP10/CXCL10 (Abcam, Cambridge, UK) antibodies. Immune complexes were detected using the Bond Polymer Refine Detection Kit according to the manufacturer's protocol (Leica, Wetzlar, Germany), then sections were counterstained with hematoxylin and eosin.

TCRγδ/T-cell intracellular antigen-1 (mouse anti-human TIA-1) (Abcam, Cambridge, UK) double staining was performed using the EnVision G/2 Doublestain System, Rabbit/Mouse (Dako), according to the manufacturer's protocol.

DNA fragmentation associated with apoptosis was detected in 4 μm tissue sections by TUNEL staining with the ApopTag Plus Peroxidase In Situ Apoptosis Kit (Millipore, Billerica, MA) according to the manufacturer's protocol.

**Statistical analysis**

*In vivo and in vitro studies:* *In vivo* experiments were performed at least twice with similar results. Survival curves were constructed using the Kaplan–Meier method and compared by log-rank test. *In vitro* data were

from three independent experiments, results were expressed as mean ± SD, statistical significance was determined by two-way analysis of variance. All analyses were performed using Graph-Pad Prism 5.0 software (Graph-Pad Software, San Diego, CA). *P* values of <0.05 were considered statistically significant.

**Immunohistochemical studies:** Variables were reported as mean ± SD. Between-group differences in vessel or cell count were assessed by one-way analysis of variance. The difference between each pair of means was evaluated using the Tukey pairwise multiple comparisons test. The SPSS software, version 11.0 (SPSS, Chicago, IL) was used, with *P* < 0.05 as the significance cut-off.

**ACKNOWLEDGMENTS**

This work has been supported by grants from Ricerca Corrente, Ministero della Salute (contributo per la ricerca intramurale) and Associazione Italiana Ricerca sul Cancro (A.I.R.C.) Milano, Italy (IG n. 13134 to E. Di Carlo) and Fondazione Cassa di Risparmio della Provincia di Chieti to E.D.C. The work was done in Genova and Chieti, Italy, Europe. The authors declared no conflict of interest.

**REFERENCES**

1. Maris, JM, Hogarty, MD, Bagatell, R and Cohn, SL (2007). Neuroblastoma. *Lancet* **369**: 2106–2120.
2. DuBois, SG, Kalika, Y, Lukens, JN, Brodeur, GM, Seeger, RC, Atkinson, JB *et al.* (1999). Metastatic sites in stage IV and IVS neuroblastoma correlate with age, tumor biology, and survival. *J Pediatr Hematol Oncol* **21**: 181–189.
3. Matthay, KK, Reynolds, CP, Seeger, RC, Shimada, H, Adkins, ES, Haas-Kogan, D *et al.* (2009). Long-term results for children with high-risk neuroblastoma treated on a randomized trial of myeloablative therapy followed by 13-cis-retinoic acid: a children's oncology group study. *J Clin Oncol* **27**: 1007–1013.
4. Seeger, RC (2011). Immunology and immunotherapy of neuroblastoma. *Semin Cancer Biol* **21**: 229–237.
5. Prigione, I, Corrias, MV, Airolidi, I, Raffaghello, L, Morandi, F, Bocca, P *et al.* (2004). Immunogenicity of human neuroblastoma. *Ann N Y Acad Sci* **1028**: 69–80.
6. Morandi, F, Levreri, I, Bocca, P, Galleni, B, Raffaghello, L, Ferrone, S *et al.* (2007). Human neuroblastoma cells trigger an immunosuppressive program in monocytes by stimulating soluble HLA-G release. *Cancer Res* **67**: 6433–6441.
7. Castriconi, R, Dondero, A, Augugliaro, R, Cantoni, C, Carnemolla, B, Sementa, AR *et al.* (2004). Identification of 4lg-B7-H3 as a neuroblastoma-associated molecule that exerts a protective role from an NK cell-mediated lysis. *Proc Natl Acad Sci USA* **101**: 12640–12645.
8. Raffaghello, L, Prigione, I, Airolidi, I, Camoriano, M, Morandi, F, Bocca, P *et al.* (2005). Mechanisms of immune evasion of human neuroblastoma. *Cancer Lett* **228**: 155–161.
9. Soldati, R, Berger, E, Zenclussen, AC, Jorch, G, Lode, HN, Salatino, M *et al.* (2012). Neuroblastoma triggers an immunoevasive program involving galectin-1-dependent modulation of T cell and dendritic cell compartments. *Int J Cancer* **131**: 1131–1141.
10. Raffaghello, L, Prigione, I, Bocca, P, Morandi, F, Camoriano, M, Gambini, C *et al.* (2005). Multiple defects of the antigen-processing machinery components in human neuroblastoma: immunotherapeutic implications. *Oncogene* **24**: 4634–4644.
11. Foreman, NK, Rill, DR, Coustan-Smith, E, Douglass, EC and Brenner, MK (1993). Mechanisms of selective killing of neuroblastoma cells by natural killer cells and lymphokine activated killer cells. Potential for residual disease eradication. *Br J Cancer* **67**: 933–938.
12. Schilbach, KE, Geiselhart, A, Wessels, JT, Niethammer, D and Handgretinger, R (2000). Human gammadelta T lymphocytes exert natural and IL-2-induced cytotoxicity to neuroblastoma cells. *J Immunother* **23**: 536–548.
13. Schilbach, K, Frommer, K, Meier, S, Handgretinger, R and Eyrich, M (2008). Immune response of human propagated gammadelta-T-cells to neuroblastoma recommend the Vdelta1+ subset for gammadelta-T-cell-based immunotherapy. *J Immunother* **31**: 896–905.
14. Pistoia, V, Bianchi, G, Borgonovo, G and Raffaghello, L (2011). Cytokines in neuroblastoma: from pathogenesis to treatment. *Immunotherapy* **3**: 895–907.
15. De Rosa, SC, Andrus, JP, Perfetto, SP, Mantovani, JJ, Herzenberg, LA, Herzenberg, LA *et al.* (2004). Ontogeny of gamma delta T cells in humans. *J Immunol* **172**: 1637–1645.
16. Morita, CT, Jin, C, Sarikonda, G and Wang, H (2007). Nonpeptide antigens, presentation mechanisms, and immunological memory of human Vgamma2Vdelta2 T cells: discriminating friend from foe through the recognition of prenyl pyrophosphate antigens. *Immunol Rev* **215**: 59–76.
17. Gober, HJ, Kistowska, M, Angman, L, Jenö, P, Mori, L and De Libero, G (2003). Human T cell receptor gammadelta cells recognize endogenous mevalonate metabolites in tumor cells. *J Exp Med* **197**: 163–168.
18. Mattarollo, SR, Kenna, T, Nieda, M and Nicol, AJ (2007). Chemotherapy and zoledronate sensitize solid tumour cells to Vgamma9Vdelta2 T cell cytotoxicity. *Cancer Immunol Immunother* **56**: 1285–1297.
19. Benzaid, I, Mönkkönen, H, Stresing, V, Bonnelye, E, Green, J, Mönkkönen, J *et al.* (2011). High phosphoantigen levels in bisphosphonate-treated human breast tumors promote Vgamma9Vdelta2 T-cell chemotaxis and cytotoxicity in vivo. *Cancer Res* **71**: 4562–4572.
20. Luckman, SP, Hughes, DE, Coxon, FP, Graham, R, Russell, G and Rogers, MJ (1998). Nitrogen-containing bisphosphonates inhibit the mevalonate pathway and prevent post-translational prenylation of GTP-binding proteins, including Ras. *J Bone Miner Res* **13**: 581–589.

21. Peng, H, Sohara, Y, Moats, RA, Nelson, MD Jr, Groshen, SG, Ye, W *et al.* (2007). The activity of zoledronic Acid on neuroblastoma bone metastasis involves inhibition of osteoclasts and tumor cell survival and proliferation. *Cancer Res* **67**: 9346–9355.
22. Bäckman, U, Svensson, A, Christofferson, RH and Azarbayjani, F (2008). The bisphosphonate, zoledronic acid reduces experimental neuroblastoma growth by interfering with tumor angiogenesis. *Anticancer Res* **28**(3A): 1551–1557.
23. Coscia, M, Quaglino, E, Iezzi, M, Curcio, C, Pantaleoni, F, Riganti, C *et al.* (2010). Zoledronic acid repolarizes tumour-associated macrophages and inhibits mammary carcinogenesis by targeting the mevalonate pathway. *J Cell Mol Med* **14**: 2803–2815.
24. Green, JR and Guenther, A (2011). The backbone of progress—preclinical studies and innovations with zoledronic acid. *Crit Rev Oncol Hematol* **77 Suppl 1**: S3–S12.
25. Gnani, M and Clézardin, P (2012). Direct and indirect anticancer activity of bisphosphonates: a brief review of published literature. *Cancer Treat Rev* **38**: 407–415.
26. Clézardin, P and Massaia, M (2010). Nitrogen-containing bisphosphonates and cancer immunotherapy. *Curr Pharm Des* **16**: 3007–2014.
27. Kondo, M, Sakuta, K, Noguchi, A, Ariyoshi, N, Sato, K, Sato, S *et al.* (2008). Zoledronate facilitates large-scale ex vivo expansion of functional gammadelta T cells from cancer patients for use in adoptive immunotherapy. *Cytotherapy* **10**: 842–856.
28. Sato, K, Kimura, S, Segawa, H, Yokota, A, Matsumoto, S, Kuroda, J *et al.* (2005). Cytotoxic effects of gammadelta T cells expanded ex vivo by a third generation bisphosphonate for cancer immunotherapy. *Int J Cancer* **116**: 94–99.
29. Bonneville, M and Scotet, E (2006). Human Vgamma9Vdelta2 T cells: promising new leads for immunotherapy of infections and tumors. *Curr Opin Immunol* **18**: 539–546.
30. Bonneville, M and Scotet, E (2006). Human Vgamma9Vdelta2 T cells: promising new leads for immunotherapy of infections and tumors. *Curr Opin Immunol* **18**: 539–546.
31. Nussbaumer, O, Gruenbacher, G, Gander, H and Thurnher, M (2011). DC-like cell-dependent activation of human natural killer cells by the bisphosphonate zoledronic acid is regulated by  $\gamma\delta$  T lymphocytes. *Blood* **118**: 2743–2751.
32. Bouet-Toussaint, F, Cabillic, F, Toutirais, O, Le Gallo, M, Thomas de la Pintièrre, C, Daniel, P *et al.* (2008). Vgamma9Vdelta2 T cell-mediated recognition of human solid tumors. Potential for immunotherapy of hepatocellular and colorectal carcinomas. *Cancer Immunol Immunother* **57**: 531–539.
33. Castella, B, Vitale, C, Coscia, M and Massaia, M (2011). V $\gamma$ 9V $\delta$ 2 T cell-based immunotherapy in hematological malignancies: from bench to bedside. *Cell Mol Life Sci* **68**: 2419–2432.
34. Nicol, AJ, Tokuyama, H, Mattarollo, SR, Hagi, T, Suzuki, K, Yokokawa, K *et al.* (2011). Clinical evaluation of autologous gamma delta T cell-based immunotherapy for metastatic solid tumours. *Br J Cancer* **105**: 778–786.
35. Morgan, G and Lipton, A (2010). Antitumor effects and anticancer applications of bisphosphonates. *Semin Oncol* **37 Suppl 2**: S30–S40.
36. Clézardin, P (2011). Bisphosphonates' antitumor activity: an unravelled side of a multifaceted drug class. *Bone* **48**: 71–79.
37. Nishio, N, Fujita, M, Tanaka, Y, Maki, H, Zhang, R, Hirotsawa, T *et al.* (2012). Zoledronate sensitizes neuroblastoma-derived tumor-initiating cells to cytotoxicity mediated by human  $\gamma\delta$  T cells. *J Immunother* **35**: 598–606.
38. Engler, S, Thiel, C, Förster, K, David, K, Bredehorst, R and Juhl, H (2001). A novel metastatic animal model reflecting the clinical appearance of human neuroblastoma: growth arrest of orthotopic tumors by natural, cytotoxic human immunoglobulin M antibodies. *Cancer Res* **61**: 2968–2973.
39. Khanna, C, Jaboin, JJ, Drakos, E, Tsokos, M and Thiele, CJ (2002). Biologically relevant orthotopic neuroblastoma xenograft models: primary adrenal tumor growth and spontaneous distant metastasis. *In Vivo* **16**: 77–85.
40. Otto, M, Barfield, RC, Martin, WJ, Iyengar, R, Leung, W, Leimig, T *et al.* (2005). Combination immunotherapy with clinical-scale enriched human gammadelta T cells, hu14.18 antibody, and the immunocytokine Fc-IL7 in disseminated neuroblastoma. *Clin Cancer Res* **11**: 8486–8491.
41. Pezzolo, A, Parodi, F, Corrias, MV, Cinti, R, Gambini, C and Pistoia, V (2007). Tumor origin of endothelial cells in human neuroblastoma. *J Clin Oncol* **25**: 376–383.
42. Hendrix, MJ, Sefror, EA, Hess, AR and Sefror, RE (2003). Vasculogenic mimicry and tumour-cell plasticity: lessons from melanoma. *Nat Rev Cancer* **3**: 411–421.
43. Carmeliet, P and Jain, RK (2011). Molecular mechanisms and clinical applications of angiogenesis. *Nature* **473**: 298–307.
44. Tammela, T and Alitalo, K (2010). Lymphangiogenesis: Molecular mechanisms and future promise. *Cell* **140**: 460–476.
45. Yamashita, J, Koi, K, Yang, DY and McCauley, LK (2011). Effect of zoledronate on oral wound healing in rats. *Clin Cancer Res* **17**: 1405–1414.
46. Groom, JR and Luster, AD (2011). CXCR3 ligands: redundant, collaborative and antagonistic functions. *Immunol Cell Biol* **89**: 207–215.
47. Russell, HV, Groshen, SG, Ara, T, DeClerck, YA, Hawkins, R, Jackson, HA *et al.* (2011). A phase I study of zoledronic acid and low-dose cyclophosphamide in recurrent/refractory neuroblastoma: a new approaches to neuroblastoma therapy (NANT) study. *Pediatr Blood Cancer* **57**: 275–282.
48. Chen, T, Berenson, J, Vescio, R, Swift, R, Gilchick, A, Goodin, S *et al.* (2002). Pharmacokinetics and pharmacodynamics of zoledronic acid in cancer patients with bone metastases. *J Clin Pharmacol* **42**: 1228–1236.
49. Di Paolo, D, Loi, M, Pastorino, F, Brignole, C, Marimipietri, D, Becherini, P *et al.* (2009). Liposome-mediated therapy of neuroblastoma. *Meth Enzymol* **465**: 225–249.
50. Morandi, F, Chiesa, S, Bocca, P, Millo, E, Salis, A, Solari, M *et al.* (2006). Tumor mRNA-transfected dendritic cells stimulate the generation of CTL that recognize neuroblastoma-associated antigens and kill tumor cells: immunotherapeutic implications. *Neoplasia* **8**: 833–842.